Journal of Environmental Management 129 (2013) 642–651

Contents lists available at ScienceDirect

Journal of Environmental Management

journal homepage: www.elsevier.com/locate/jenvman

Kinetics of cadmium(II) uptake by mixed maghemite-magnetite nanoparticles

Saidur Rahman Chowdhury*, Ernest K. Yanful [1]

Department of Civil and Environmental Engineering, University of Western Ontario, London, ON N6A 5B9, Canada

ARTICLE INFO

Article history:
Received 23 October 2012
Received in revised form
30 July 2013
Accepted 10 August 2013
Available online 16 September 2013

Keywords:
Cadmium
Adsorption
Kinetics
Mixed magnetite–maghemite and X-ray photoelectron spectroscopy (XPS)

ABSTRACT

In the present study, batch adsorption experiments involving the adsorption of Cd(II) ions from aqueous solutions have been carried out using mixed maghemite-magnetite as adsorbent. The uptake capacity of Cd(II) ions by mixed maghemite-magnetite increased with an increase in the pH of the adsorbate solution. An increase in adsorbent dosage increased Cd(II) removal but decreased adsorption capacity and it was found to follow the pseudo-second-order model. Cd removal from a solution containing 1.5 mg/L initial concentration of Cd(II) decreased from 1.9 to 1.3 mg/g upon increasing the temperature from 10 to 50 °C. Cadmium adsorption may be partly diffusion controlled and partly due to electrostatic effect along with specific adsorption involving the adsorption of Cd^{++} and $CdOH^{+}$ on mixed maghemite-magnetite nanoparticles in the alkaline pH range. X-ray photoelectron spectroscopy (XPS) surveys confirmed that Cd^{2+} ions may undergo oxidation-reduction reactions upon exposure to mixed maghemite-magnetite, or may be fixed by complexation to oxygen atoms in the oxyhydroxy groups at the surface of the iron oxide nanoparticles. After Cd(II) adsorption by the maghemite-magnetite mixture, the percent maghemite decreased from 74.8 to 68.5%.

1. Introduction

Cadmium, a toxic heavy metal, is relatively a less abundant metallic element and one of the non-essential substances released to the environment through anthropogenic activities including the combustion of fossil fuels, metal production, application of phosphate fertilizers, electroplating and the manufacturing of batteries, pigments, and screens (Sharma, 2008; Marin et al., 2007). According to Waalkes (2000) and Sharma (2008), cadmium is reportedly a potent carcinogen and teratogen impacting lungs, kidneys, liver and reproductive organs. According to WHO (2008) guideline, the maximum cadmium concentration in drinking water is 0.003 mg/L. Singh et al. (1998) reported that cadmium has toxic effects when its concentration exceeds the threshold limit value (TLV) of 0.005 mg/L and causes different types of acute and chronic disorders.

The conventional methods for treating wastewaters containing cadmium involve alkaline precipitation and ion exchange. However, due to high maintenance costs, these methods do not suit the needs of many developing and emerging economies such as India (Naidu et al., 1994). These authors further reported that out of the available treatment methods, adsorption was selected because of its sludge-free clean operation and the feasibility of using a variety of adsorbents, such as activated carbon discarded automotive tyres, agricultural products and by-products, and starch Xanthate, for cadmium removal. A variety of adsorbents, including clays, zeolites, dried plant parts, agricultural waste biomass, biopolymers, metal oxides, microorganisms, sewage sludge, fly ash, activated carbon, magnetite and hematite have been used for cadmium removal (Mahalik et al., 1995; Singh et al., 1998; Alloway and Steinnes, 1999; Cornell et al., 2003; Marin et al., 2007; Tan and Xiao, 2009). Singh et al. (1998) reported that the maximum Cd removal by hematite was 98% at a cadmium concentration of 44.88 μmol/L, a temperature of 20 °C and pH 9.2 with 40 g/L of hematite of particle size <200 μm and equilibrium contact time, 2 h. Magnetite can also adsorb cadmium (Cd), cobalt, chromium and arsenic from aqueous solution (Cornell et al., 2003). The controlling mechanism of the adsorption process is generally a function of the standard redox potential of the contaminant metal. The standard redox potential of Cd^{2+} (−0.2 to −0.40 V, 25 °C) is very close to that of iron oxide (−0.25 to −0.45 V, 25 °C), and thus, the removal of Cd^{2+} ions by iron oxide is due to sorption (Pang et al., 2007; Geological Survey of Japan, 2005).

* Corresponding author. Tel.: +1 5194339386; fax: +1 519 661 3942.
E-mail addresses: saidurc@yahoo.com (S.R. Chowdhury), eyanful@uwo.ca (E.K. Yanful).
[1] Tel.: +1 519 661 4069.

0301-4797/$ – see front matter © 2013 Elsevier Ltd. All rights reserved.
http://dx.doi.org/10.1016/j.jenvman.2013.08.028

Boparai et al. (2009) found that the maximum Cd uptake capacity of Zero-Valent Iron (nZVI) for Cd^{2+} was 769.2 mg g^{-1} at pH 8.5 and 297 K. These authors showed further that the adsorption process was endothermic, spontaneous and chemisorptive. However, there has been limited use of nZVI in site remediation because of its extremely reactive nature, improper handling during application and its toxicity (Li et al., 2009; Phenrat et al., 2009; Chowdhury et al., 2012). These authors further reported that nZVI produces highly reactive and unstable molecule free radicals through the transformation process. These free radicals need additional electrons for stabilization in any system and can effect antioxidant enzymatic activities, peroxidation of membrane lipids, modification of nucleic acids, and eventually cause cell death and tissue injury. Gavaskar et al. (2005) noted that the toxicity of the potential by-products needs to be considered when assessing the pros and cons of using nZVI for remediation. If the contaminant cannot be completely degraded by nZVI and the by-products formed in the system pose a greater environmental hazard than the original target contaminant, then the application of nZVI in site remediation might not be the best solution.

The objective of the present work is to investigate the adsorption kinetics of cadmium removal by mixed iron oxide nanoparticles (γ-Fe_2O_3–Fe_3O_4). Sorption kinetics was examined to develop an understanding of the rate and the controlling mechanisms (e.g., surface versus intraparticle diffusion) of sorption. Kinetic data can be used to predict the rate at which the target contaminant is removed from solution. The results from the study can be used to assess the utility of mixed maghemite-magnetite nanoparticles for heavy metal removal, in particular cadmium adsorption, at the field scale. This is one of the very few studies that have, to date, investigated the feasibility of Cd(II) removal from aqueous solution by mixed maghemite-magnetite (γ-Fe_2O_3–Fe_3O_4) nanoparticles. It is probably more realistic to evaluate the removal efficiency of the mixture because, in nature, these minerals commonly occur together. The identification of the chemical states of the adsorbed Cd using XPS analysis was a major contribution of the study. Theoretical multiplet analysis of the Cd adsorbed γ-Fe_2O_3–Fe_3O_4 presented in the study is a novel contribution to the literature on XPS studies. In addition, no published study has, to date, examined the effect of contact time, pH, solid/liquid ratio and temperature on the adsorption and distribution coefficient of Cd on mixed γ-Fe_2O_3–Fe_3O_4 surfaces.

2. Materials and methods

2.1. Characterization of the adsorbent

Magnetite nanoparticles were purchased from Reade Advanced Materials (Rhode Island, U.S.A.). The size range for this commercial grade 'magnetite' was 20–80 nm. The sample arrived in powder form in an airtight plastic bag. Pre-adsorption laboratory characterization of the sample, however, showed that the sample was actually a mixture of maghemite and magnetite nanoparticles. The surface area of the sample was determined using the N_2 adsorption method and applying the Brunauer, Emmett, Teller (BET) equation and found to have an average value of 49.5 m^2/g. Further examination and characterization of the sample showed that the particles were dispersed and contained 99.9% pure 20–80 nm magnetite-maghemite particles that had a black and spherical morphology and a bulk density of 0.8 g/cm^3. X-ray photoelectron spectroscopy analysis confirmed that the mixed oxide (γ-Fe_2O_3–Fe_3O_4) comprised 74.8% maghemite (γ-Fe_2O_3) and 25.2% magnetite (Fe_3O_4) (Fig. 10a).

2.2. Reagents

Stock solutions of cadmium (Cd) were prepared by dissolving a hydrated cadmium nitrate salt ($Cd(NO_3)_2.4H_2O$) in distilled water. Certified reagent grade chemicals were used to prepare all solutions for the experiments without further purification. Glass volumetric flasks and reaction vessels were treated with 10% HNO_3 and rinsed several times with de-ionized water before they were used.

A known amount (0.8 g/L) of maghemite-magnetite sample was added to a desired concentration of stock (Cd) solution in plastic bottles. Solutions were prepared with de-ionized water. Standard acid (0.1 M HNO_3) and base (0.1 M NaOH) solutions were used for pH adjustment. The pH of each solution was measured using an Orion combination electrode. In the batch test, Cd concentrations were kept in the range of 0.2–1.5 mg/L.

2.3. Batch adsorption procedure

Batch adsorption experiments were carried out by agitating 0.2 g of the adsorbent (20–80 nm mixed maghemite-magnetite particles) with 250 mL aqueous solution of cadmium of desired concentration, temperature, pH, and ionic strength in different polyethylene bottles on a shaking thermostat at 100–120 rpm. After predetermined time intervals, the adsorbent was separated from solutions by centrifugation. Adsorption was determined by measuring the concentration of cadmium (Cd) left in the aliquot by ICP-OES (inductively coupled plasma-optical emission spectroscopy). The pH of the solutions was maintained at the desired value by the addition of either 0.1 M HNO_3 or 0.1 M NaOH. In equilibrium and thermodynamic studies, experiments were carried out at different temperatures with solutions of different concentrations of cadmium. The experiments were carried out in triplicate and the mean values were reported. The results were found to vary within ±5%. The standard deviation of each point on the graphs was calculated. The resulting error bars representing standard deviation for the figures were found to be small. Blank experiments (distilled water plus adsorbent alone) did not reveal any detectable Cd adsorption by the adsorbent. The supernatant solutions were separated and solid samples were dried in a vacuum desiccator. The dried Cd adsorbed maghemite-magnetite nanoparticles were kept in an airtight ceramic dish to prevent any reaction with air.

2.4. Instrumentation for XPS

All spectra were collected using a Kratos Axis Ultra X-ray Photoelectron Spectrometer (XPS). The samples were analyzed using a monochromatic Al Kα X-ray source (15 mA, 14 KV) and chamber pressures of 10^{-7}–10^{-6} Pa. The resolution function of the XPS instrument was found to be 0.35 eV using silver Fermi edge (Grosvenor et al., 2004), During the experiments, a charge neutralizer filament was used to control or minimize charging of the samples. The following conditions were used in the survey scans: energy range = 0–1100 eV, pass energy = 160 eV, step size = 0.7 eV, sweep time = 180 s and X-ray spot size = 700*400 μm. An energy range of 20–40 eV was used for the high-resolution spectra, depending on the peak being examined. The sampling volume of the XPS for a 10 nm depth of penetration and a slot of 700 microns by 160 microns was approximately 100 cubic microns. The photons interact with atoms in the surface region, causing electrons to be emitted by the photoelectric effect. XPS spectral lines are identified after the ejection of electron from the shell (1s, 2s, 2p, etc.). The ejected photoelectron has electron Binding Energy (BE):

$$BE = h\nu - E_k - \Phi \quad (2.1)$$

Where: BE = Electron Binding Energy; E_k = Electron Kinetic Energy; Φ_{spec} = Spectrometer Work Function. Each electron contains its binding energy. By knowing this binding energy one can identify the element from which the energy is coming. An important advantage of XPS is that it is capable of providing information on chemical states from the variations in binding energies, or chemical shifts, of the photoelectron lines. All dried samples were transferred into the spectrometer via a glove box filled with N_2 (g) or Ar (g). This was done to minimize the exposure of the samples to air or airborne impurities. In order to provide fresh and clean mineral faces for the analysis, the dried samples were fractured in a vacuum prior to the analysis.

2.5. Theory

2.5.1. The distribution coefficient K_D

The uptake distribution coefficient, K_D, in Equation (2.2) is defined as the concentration of the species adsorbed per gram of the sorbent divided by its concentration per L in the liquid phase:

$$K_D = (C_i - C_{eq})V/C_{eq}m(L/g) \quad (2.2)$$

Here, V is the volume of the solution in L and m is the mass of sorbent in g.

2.5.2. Pseudo first-order equation

The pseudo first-order equation for any chemical system can generally be illustrated as (Lagergren, 1898):

$$dq_t/dt = k_{lads}(q_e - q_t) \quad (2.3)$$

where q_e and q_t represent the adsorption capacities (mg/g) at equilibrium and at time t, respectively, and k_{1ads} is the rate constant for pseudo first-order adsorption (min^{-1}). After integration and considering the boundary and initial conditions, $t = 0$ to $t = t$ and $q_t = 0$ to $q_t = q_t$, Eq. (2.3) can be expressed as:

$$Log(q_e - q_t) = Logq_e - k_{lads}{}^{*}t/2.303 \quad (2.4)$$

2.5.3. The pseudo second-order equation

According to Ho et al. (2000), the pseudo second-order adsorption kinetic rate equation may be illustrated by Equation (2.5):

$$dq_t/dt = k_{2ads}(q_e - q_t)^2 \quad (2.5)$$

where, k_{2ads} indicates the rate constant of pseudo second-order adsorption ($g^{*}mg^{-1}{}^{*}min^{-1}$). Applying the boundary conditions $t = 0$ to $t = t$ and $q_t = 0$ to $q_t = q_t$, the integrated form of Eq. (2.5) can be reduced to Equation (2.6):

$$1/(q_e - q_t) = 1/q_e + k_{2ads}{}^{*}t \quad (2.6)$$

which is the integrated rate law for a pseudo second-order reaction. Eq. (2.6) can be re-arranged to give Eq. (2.7):

$$t/q_t = 1/k_{2ads}tq_e^2 + t/q_e \quad (2.7)$$

If the initial adsorption rate, h ($mg^{*}g^{-1}$ min^{-1}) is:

$$h = k_{2ads}{}^{*}q_e^2 \quad (2.8)$$

then Eqs. (2.7) and (2.8) can be expressed as:

$$t/q_t = 1/h + t/q_e \quad (2.9)$$

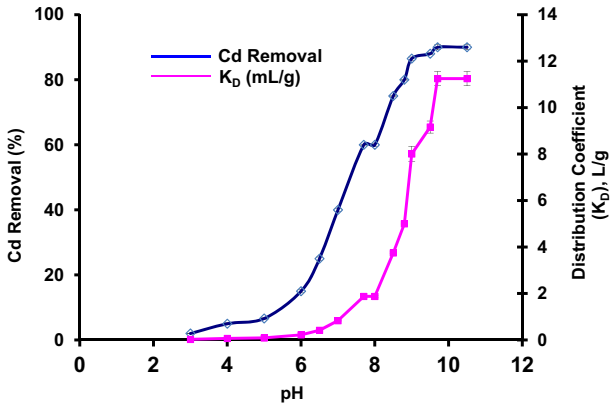

Fig. 1. The effect of pH on Cd removal (%) and uptake distribution coefficient (K_D). Operating conditions: contact time = 120 min, $T = 22 \pm 0.5$ °C, $S/L = 0.8$, Co = 1.5 mg/L.

2.5.4. The intraparticle diffusion model

The intraparticle diffusion model was illustrated by Srivastava et al. (1989) and Weber and Asce (1963):

$$Y_{id} = k_{id}(t)^a \quad (2.10)$$

A linearized form of the equation can be expressed by

$$logY_{id} = logK_{id} + alogt \quad (2.11)$$

where, Y_{id}, t, a and k_{id} represent the percent chemical species adsorbed, the contact time (min), the gradient of linear plots and the intra-particle diffusion rate constant (min^{-1}), respectively. The value of a also depicts the adsorption mechanism and k_{id} is considered a rate factor, i.e., percent adsorbate adsorbed per unit time.

2.6. Equilibrium adsorption isotherm

The experimental data calculated at room temperature were applied to the linearized forms of Langmuir and Freundlich [Eqs. (2.12) and (2.13), respectively], which were suitable for determining adsorption as well as to find out the nature of adsorption of adsorbate on adsorbent.

$$C_e/q_e = 1/bq_m + C_e/q_m \quad (2.12)$$

$$Logq_e = LogK + (1/n{}^{*}LogC_e) \quad (2.13)$$

where C_e and q_e are equilibrium solute concentration (mg/L) and equilibrium adsorption capacity (mg/g), respectively. The other parameters, q_m, b and n are isotherm constants that represent maximum adsorption capacity (mg/g), energy of adsorption (L/g) and adsorption intensity respectively.

3. Results and discussion

3.1. Parameters affecting the removal of cadmium

3.1.1. Effect of pH and distribution coefficient (K_D)

Batch experiments were conducted at different pH to determine the optimum condition for Cd(II) removal by mixed maghemite-magnetite nanoparticles. The distribution coefficient, K_D increased with increasing pH and the maximum K_D was observed at a pH of approximately 9.3 (Fig. 1). It is clear from Fig. 1 that the adsorption of cadmium is higher in the alkaline pH range of 8.0–10.0 than in the acid range. The standard deviation of each point on the graph

was calculated, as shown in Fig. 1. The maximum standard deviation for 90% Cd removal was ±0.8 while the maximum standard deviation for distribution coefficient (K_D) was found to be ±0.3. Removal is very small in the acidic range and reaches a maximum at approximately pH 9.3. In a highly acidic medium, there is a chance of dissolution of the adsorbent (Stumn, 1987) and a consequent decrease in the number of active sites. In addition to this effect, the adsorbent surface is highly protonated in acidic medium which is not favorable for cadmium uptake because in such medium, Cd(II) is the dominant ion (Singh et al., 1998). As a result, the adsorption of cadmium is hindered due to electrical repulsion. As pH increases, the degree of protonation of the surface reduces gradually and approaches zero at pH 7.0 resulting in a gradual increase in adsorption. Above pH 8.0, where Cd^{2+} and $CdOH^{+}$ species are present in solution (Singh et al., 1998; Geological Survey of Japan, 2005), the adsorbent surface starts taking up a net negative charge creating an electrostatically favorable environment for higher cadmium uptake. Thermodynamic calculations show that different hydroxyl forms of the Cd ion can be observed depending on the pH of the solution. These forms include $Cd(OH)^{+}$, $Cd(OH)_2$, $Cd(OH)_3^-$ and $Cd(OH)_4^{2-}$ for Cd (Geological Survey of Japan, 2005). Within the pH ranges measured in the present adsorption experiments, Cd is expected to be dominantly present in its divalent ionic forms.

The functional groups of iron oxides consist of surface hydroxyl groups that usually arise from water adsorption or from structural OH. The surfaces of metal oxides in aqueous solution are generally attached with hydroxyl groups that can change in form at different pH values. These groups contain a double pair of electrons together with a dissociable hydrogen atom that can generate suitable conditions for them to react with both acids and bases. The charge on the iron oxide surface dominates the adsorption or desorption of protons and it is generated by the dissociation (ionization) of the surface hydroxyl groups depending on the pH of the solution. Cornell et al. (2003) have noted that magnetite will produce Fe^{2+} and its hydrolysis products ($FeOH^{+}$, $Fe(OH)_2^0$, and $Fe(OH)_3^-$), depending on solution pH. They further reported that acidity constant, pKa, values for most iron oxides are usually between 5 and 10. The mixed maghemite-magnetite used in the present study consists of two types of iron oxides, γFe_2O_3 and Fe_3O_4. Thus, the abundance of Fe^{2+} or Fe^{3+} and the hydrolysis products of Fe^{2+} would influence the acidity constants of a specific surface group. Cornell et al. (2003) also reported that the acidity constant, pKa_1, of magnetite (25.2% of the adsorbent used in the present study), is 5.6. At pH greater than 5.6, the dominant functional groups at the iron oxide surface are $Fe(OH)_2^0$, and $Fe(OH)_3^-$. Moreover, most iron oxide surfaces hold the dominant functional groups of Fe^{2+} or $FeOH^{+}$ when solution pH is acidic, and $Fe(OH)_2^0$ and $Fe(OH)_3^-$ when basic. Thus, it is clear that iron oxide attracts positive Cd(II) species at high pH. The hydroxyl groups on the iron oxide surface at high pH are $Fe(OH)_2^0$, and $Fe(OH)_3^-$ which enhance the attraction of positively charged Cd(II) species at the higher pH value. The oxidation of magnetite produces maghemite (Chowdhury et al., 2012). Therefore, hydrated ferric oxide (HFO) nanoparticles can be produced by Fe(III) compound in aqueous solution. Adsorption would keep Cd(II) on the maghemite-magnetite surface through a Lewis acid base (LAB) interactions and iron oxide surfaces would coordinate with hydroxyl ions or water molecules that share their lone electron pair with Fe surface (Cornell et al., 2003). Thus, surface Fe atoms behave like Lewis acids in aqueous solution that react with Lewis bases (e.g. water). Cornell et al. (2003) further noted that the surface hydroxyl groups of the iron oxides in an aqueous environment work as a chemically reactive entities at the surface of the solid. These surface properties allow them to react with acid and bases. Fig. 1 shows the percent removal and uptake distribution

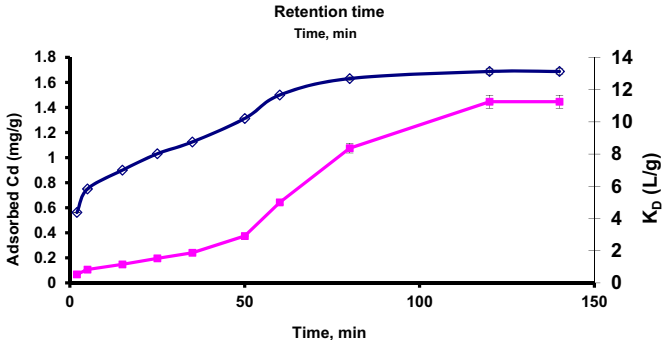

Fig. 2. The effect of contact time on Cd(II) removal by mixed maghemite-magnetite. Conditions: Particle size: 20–60 nm, Temperature: 22 ± 0.5 °C and initial concentration: 1.5 mg/L.

coefficient (K_D) of Cd(II) in the solution after adsorption at different pH values and the results show high pH dependency during Cd(II) removal by mixed maghemite-magnetite particles. A maximum adsorption or removal efficiency of 90% was found at pH 9.3 and the adsorbed amount was 1.69 mg/g for an initial Cd(II) concentration of 1.5 mg/L. The affinities of the maghemite-magnetite for the different species of Cd(II) existing at different pH values, namely Cd^{2+} and $CdOH^{+}$ (Singh et al., 1998; Geological Survey of Japan, 2005), may be different and attributable to the variation in removal efficiency at pH values above 8. From potentiometric titrations, it was found that the surface of magnetite particles had a positive surface charge up to pH 6.8, the point of zero charge, and a negative surface charge in the pH range 6.8–9.5 (Yean et al., 2005). Tuutijärvi et al. (2009) found that maghemite had a point of zero charge at pH_{pzc} 7.5 and the more alkaline the condition the more negative was the surface charge of the adsorbent and, accordingly, the more attractive to positive Cd(II) species at higher pH. Thus, it was postulated that mixed maghemite-magnetite particles can adsorb either negatively or positively charged metal species by electrostatic attraction as well as by redox reaction depending on pH.

The possibility of Cd^{2+} precipitation was also investigated. Since the system contained mixed iron oxides and cadmium nitrate solution, the only anions that could precipitate with Cd^{2+} at high pH were OH^- and NO_3^-. Geochemical equilibrium calculations using MINTEQA2 or PHREEQC gave negative saturation indices for Cd solids (for example, $Cd(OH)_2$), indicating that the solution was undersaturated with respect to these solids. From these results, it can be concluded that Cd^{2+} did not precipitate, but was instead adsorbed. In fact, a number of researchers (Moore and Ramamoorthy, 1984; Singh et al., 1998; Geological Survey of Japan, 2005) have noted that cadmium would not precipitate at pH less than 9.5 when the solution contains very low Cd concentration.

3.1.2. Time of equilibrium

The kinetics of Cd(II) adsorption was studied by varying the contact time between maghemite-magnetite and the respective solution from 10 to 140 min using 0.8 g/L adsorbent at a Cd concentration of 1.5 mg/L and pH 9.3. Batch adsorption experiments were carried out in order to find the optimum retention time. The results showed that the sorption efficiency increases rapidly and more than 75% of the adsorbed Cd occurred within 60 min when a solid–liquid ratio of 0.8 was used. The rapid uptake of Cd(II) by mixed maghemite-magnetite nanoparticles is perhaps due to external surface sorption, which is different from microporous adsorption. Although nearly all the adsorption sites of maghemite–

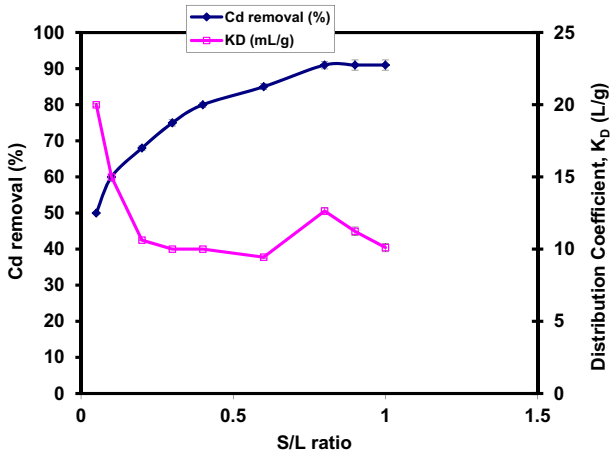

Fig. 3. Uptake distribution co-efficient K_D and the Cd removal percentage (%) at different solid–liquid ratio.

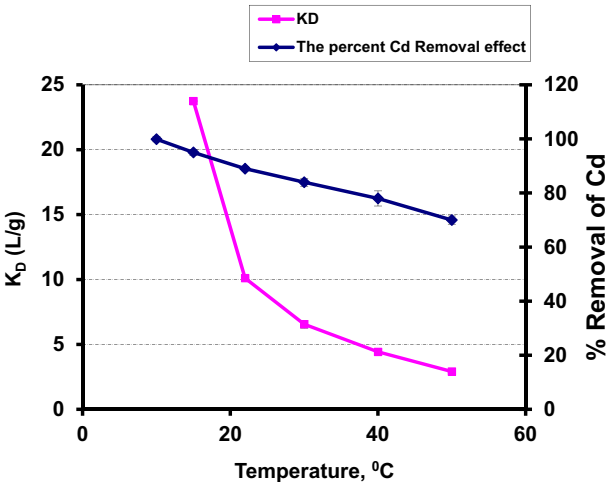

Fig. 4. Uptake distribution coefficient K_D and Cd removal percentage (%) at different temperature. (Temperature ranges: 10° to 50 °C, $S/L = 0.8$ and $C_0 = 1.5$ mg/L).

magnetite nanoparticles are present in the exterior of the adsorbent compared to the porous adsorbent, it is easy for the adsorbate to contact these active sites, thus resulting in a rapid approach to equilibrium. The current study illustrates that 120 min are needed to reach equilibrium. Fig. 2 presents the adsorption and uptake distribution coefficient (K_D) of Cd on mixed maghemite-magnetite nanoparticles. In Fig. 2, the range of standard deviations for the adsorbed Cd concentration (mg/g) was found to be very small, that is, ±0.002 to ±0.025.

Cd uptake increases with elapsed time and reaches equilibrium in 2 h for the initial concentration of 1.5 mg/L. Such observations were also noted at various pH values and temperatures of the system with the 20–60 nm adsorbent particles. However, the uptake of cadmium from water by mixed maghemite-magnetite depended on the initial concentration of cadmium. The maximum removal was found to be 1.68 mg/g or 90% at an initial concentration of 1.5 mg/L and maghemite-magnetite nanoparticle concentration of 0.8 g/L. The distribution coefficient, K_D, increases with increasing contact time and the maximum K_D was found to be 11.25 L/g after 2 h (Fig. 2).

The process was not spontaneous and it took 2 h to complete the adsorption under the given conditions. There are three possible reasons for this. First, Cd(II) species may transfer from the bulk fluid phase to the outer particle surface of the adsorbent for contact (film diffusion). Second, the Cd species can migrate within the micro and macro pores of the mixed maghemite-magnetite particles (intra-particle diffusion) (Singh et al., 1998). Finally, there might be electrostatic attraction or reaction occurring between adsorbate (Cd(II) species) and adsorbent.

3.1.3. Effect of solid/liquid ratio (S/L) and distribution coefficient (K_D)

The operating conditions used were: initial cadmium concentration = 1.5 mg/L, pH 9.3 and $T = 22 \pm 0.5$ °C. The solid/liquid (S/L) ratio was varied from 0.1 to 1. Fig. 3 shows the effect of S/L ratio on the adsorption of cadmium. It can be seen that the percentage cadmium adsorption increased at the high S/L ratio. This is due to an increasing surface area at a high S/L ratio. The resulting standard deviations were small, as indicated by the error bars in Fig. 3. The standard deviations for the Cd removal (%) at S/L ratios of 0.8, 0.9 and 1.0 were calculated to be ±0.25, ±0.3 and ±0.3 respectively.

The distribution coefficient, K_D, showed the reverse trend (Fig. 3) for different concentrations of adsorbents during the removal of Cd(II). Similar results were reported by Barkat et al. (2009). In the experimental conditions used in the present study, the surface of mixed maghemite-magnetite contained negative hydroxyl groups (OH^-) that were likely replaced by positive Cd–O ligands. The adsorption capacity (Fig. 3) was found to be almost 91% or 1.7 mg/g when the S/L ratio and K_D were 0.8 and 12.63 L/g, respectively. In Equation (2.2), the mass of adsorbent, m, increases with S/L ratio, which results in a decrease in K_D value. The Cd removal was found to be constant beyond an adsorbent concentration of 0.8 g/L, although the adsorbent concentration (m, the denominator in Equation (2.2)) increased with S/L. This would explain the observed reverse trend in the distribution coefficient, K_D (Fig. 3).

3.1.4. Effect of temperature on Cd removal

Santiago et al. (2012) found that the point of zero charge for magnetite particles depends on the solution temperature. They further reported that pH_{pzc} decreased from 7.1 to 6.5 when the solution temperature was increased from 0 to 50 °C. Since the point of zero charge of iron oxides does not vary significantly in the temperature range of 10–50 °C, the change in protonation/deprotonation (acidity) constants of the surface groups would be negligible in the case of Cd adsorption on mixed maghemite-magnetite. Cornell et al. (2003) and Chowdhury et al. (2012) found the pH_{zpc} of mixed iron oxide to be 6.8–7.5 depending on temperature.

In the present study, the effect of temperature on Cd(II) adsorption by mixed maghemite-magnetite was examined from 10° to 50 °C at pH 9.3, $S/L = 0.8$ and $C_0 = 1.5$ mg/L. The removal of Cd from a solution containing 1.5 mg/L initial concentration of Cd(II) decreased from 1.9 to 1.3 mg/g upon increasing the temperature from 10 to 50 °C.

Fig. 4 shows the effect of temperature on distribution coefficient and percent Cd removal by 20–60 nm mixed maghemite–magnetite nanoparticles. The resulting standard deviation on the graph was found to be very small. As indicated, percent removal decreases with increase in temperature. During Cd(II) removal, the distribution coefficient was 1248.75, 23.75,10.11, 6.5, 4.4, and 2.9 L/g at 10, 15, 22, 30, 40 and 50 °C, respectively. In other words, the distribution coefficient decreased from 1248.75 to 2.9 L/g, as shown in Fig. 4. The percent Cd(II) removal also showed a decreasing trend, that is, 99.9% removal was found at 10 °C while almost 70% removal was observed at 50 °C. This indicates the exothermic nature of the process. The decrease in percent removal may be attributed to a relative increase in the escaping tendency of the solute from the

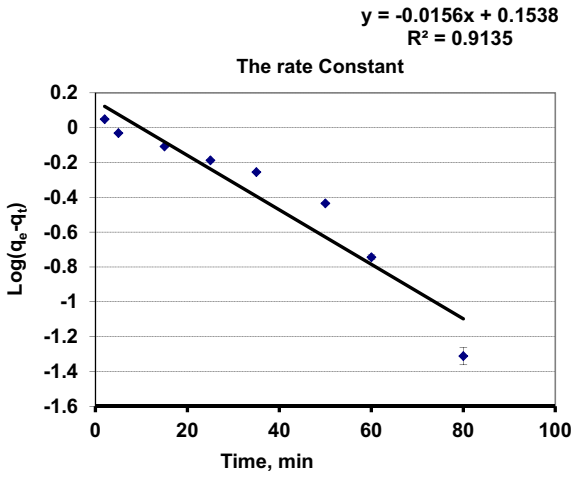

Fig. 5. The rate constant of pseudo-first order adsorption k_{1ads} and the amount of Cd(II) ion adsorbed at equilibrium, q_e.

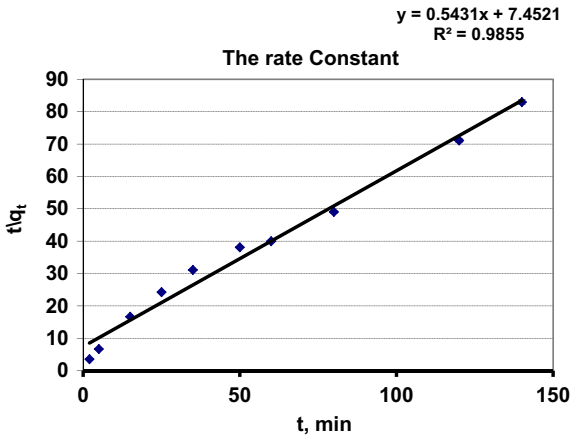

Fig. 6. The rate constant of pseudo-second order adsorption k_{2ads} and the amount of Cd(II) ion adsorbed at equilibrium, q_e.

solid phase to the bulk phase with the increase in solution temperature. The distribution coefficient, K_D varied in the same way (Fig. 4).

3.2. Adsorption kinetics study

The adsorption kinetics study explains the solute sorption rate. It is obvious that this rate controls the residence time of adsorbate adsorption at the solid–solution interface. The adsorption of Cd on mixed maghemite-magnetite is not an instantaneous process because the Cd species have to diffuse from the solution to the surface of the mixed maghemite-magnetite, and then to the internal surface areas. The overall rate of approach of this process to equilibrium delineates the sorption kinetics. The kinetics of Cd(II) sorption on the mixed maghemite-magnetite was investigated using pseudo first-order, pseudo second-order and intraparticle diffusion kinetic models. The closeness of the experimental data and the model predicted values were expressed by the correlation coefficients (R^2, values close or equal to 1). The relatively high R^2 value implies that the model successfully illustrates the kinetics of Cd(II) adsorption.

3.2.1. Pseudo first-order equation and the pseudo second-order equation

Experimental data were fitted with the pseudo first-order and second-order equations to determine the reaction rate constant (k_{1ads}) of Cd removal by mixed maghemite-magnetite nanoparticles. Eq. (2.4) represents pseudo first-order equation. This equation means that the values of $\log(q_e - q_t)$ are linearly correlated with t. Thus a plot of $\log(q_e - q_t)$ versus t should give a linear relationship if the reaction follows first-order. The values k_{1ads} and q_e can be determined from the slope and intercept of the plot (Fig. 5). Fig. 5 shows that the maximum standard deviation on the graph is ±0.05. The experimental data produced a trend line with correlation coefficient of $R^2 = 0.91$. From the plot, k_{1ads} was found to be 3.6×10^{-2} min^{-1}.

Similarly, Eq. (2.9) represents pseudo second-order equation. A plot of (t/q_t) against t in Eq. (2.9) should yield a linear relationship from which q_e and k_{2ads} can be calculated from the slope and intercept of the model Equation (2.9). In Fig. 6, the resulting standard deviation is very small. The value of k_{2ads} was found from the plot to be 3.96×10^{-2} g/mg*min. The adsorption kinetics data were modeled using the pseudo first order and pseudo-second order kinetic equations. It is seen from the results that the pseudo second-order adsorption kinetic equation is a better sorption kinetics model than the pseudo first-order kinetic equation, since it gave a better fit with the experimental data (correlation coefficient, $R^2 = 0.99$).

3.2.2. The intraparticle diffusion model

The intraparticle diffusion model was demonstrated by Srivastava et al. (1989) and Weber and Asce (1963). The application of the intraparticle diffusion model (shown in Equation (2.11)) to the experimental data in the present study gave a good fit plot with a correlation coefficient, $R^2 = 0.98$ and a value of "a" that is less than unity (0.27). This supports an enhanced rate of adsorption (Srivastava et al., 1989; Erhan et al., 2004; Barkat et al., 2009) which, in turn, is linked to improved bonding. The resulting R^2 values (average 0.98) also show that the intra-particle diffusion process may be the rate-limiting step (Barkat et al., 2009). Thus, higher values of k_{id} demonstrate an enhancement of adsorption (Erhan et al., 2004), indicating a better adsorption mechanism that facilitates bonding between Cd(II) ions and adsorbent particles. The value of k_{id} (also considered as a rate factor, i.e., percent Cd(II) adsorbed per unit time) was estimated to be 24.56 min^{-1} from the slope of such plots (Fig. 7). Thus, it may be assumed that the adsorption of cadmium is partly diffusion controlled and partly due to an electrostatic effect along with specific adsorption involving the adsorption of Cd^{++} and $CdOH^{+}$ on mixed maghemite–magnetite nanoparticles in the alkaline pH range (Singh et al., 1998).

3.3. Adsorption isotherms

Adsorption of Cd(II) by mixed maghemite-magnetite nanoparticles was modeled using the Freundlich and Langmuir isotherms and the best fit was assessed using the correlation coefficient (R^2). According to Yang (1998), the Freundlich isotherm is applicable to both monolayer (chemisorption) and multilayer (physisorption) whereas the Langmuir isotherm assumes only monolayer (chemisorption) adsorption on a uniform surface with a finite number of adsorption site.

In this study, the adsorption data were fitted with the Langmuir and Freundlich adsorption equation to identify adsorption parameters for future modeling and scale up. The calculated linear regression coefficient (R^2) values from the Langmuir and Freundlich equations (as shown in Fig. 8) are found to be 0.9931 and 0.98 respectively indicating the applicability of the Langmuir adsorption isotherm to this adsorbate-adsorbent system. The constants, q_m and

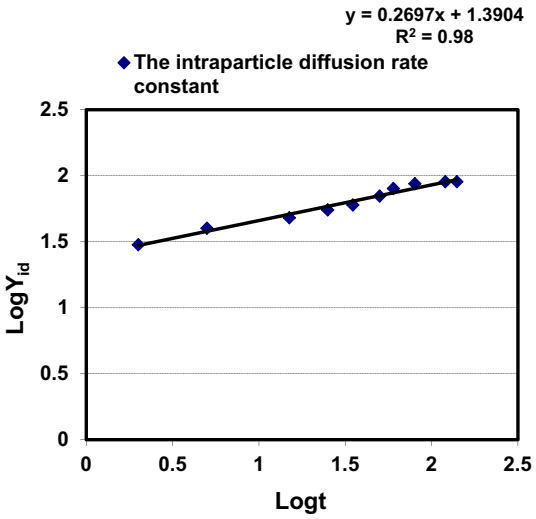

Fig. 7. Determination of the intra-particle diffusion rate constant, k_{id} (min^{-1}) during Cd(II) removal by mixed maghemite-magnetite.

b, were determined from the slope and intercept of plot of C_e/q_e versus C_e, at room temperatures. The Cd^{2+} adsorption capacity on absorbent at room temperature (295 K) was 2.7 mg g^{-1}. The Cd^{2+} adsorption capacities of other adsorbents reported in the literature are as follows: activated carbon (3.37 mg/g), hematite (4.94 mg/g), wheat stem (11.6 mg/g), chitin (14.7 mg/g), and bamboo charcoal (12.08 mg/g) (Boparai et al., 2009; Wang et al., 2010).

As indicated, the data (R^2 value more than 0.99) show that adsorption by maghemite-magnetite nano-particles is well described by the Langmuir isotherm. Thus, from the isotherm equation, it is apparent that maghemite-magnetite nanoparticles are very useful adsorbent for Cd(II) uptake from aqueous solution.

3.4. Multiple linear regression modeling of the Cd adsorption data

The simultaneous effect of several independent variables, such as pH, contact time, *S*/*L* ratio and temperature on the dependent variable, percentage Cd removal was modeled using multiple regression analysis (MRA) and statistical computation software, *R*. The results are presented in Tables 1 and 2. These results show that the independent variables have a significant effect ($p < 0.05$) on the percentage removal of Cd by mixed maghemite-magnetite nano-particles. Using these data, the following model has been suggested to predict the uptake of Cd under given conditions:

$$Y = 21.2095799X_1 + 0.299232X_2 + 42.2337443X_3 - 0.75027340X_4 - 165.09903 \quad (3.1)$$

Where, *Y* indicates the percentage removal of Cd and X_1, X_2, X_3 and X_4 represent the sample pH, contact time in minute, solid–liquid ratio and temperature (°C) of the system respectively. Tables 1 and 2 demonstrate the model values estimated using Eq. (3.1) and the experimental values. The results show that the coefficients for pH, contact time and *S*/*L* ratio are highly significant at 0.1% level ($p < 0.001$) while the coefficient of temperature is significant at 1% level ($p < 0.01$). This indicates that pH, contact time and S/L have greater effect on cadmium removal than temperature. The model shows that increase in temperature (X_4) would decrease the removal efficiency (*Y*) under the given conditions. The overall *F*-test and *t*-test also support the significance level of the different independent variables in the proposed model. The multiple correlation coefficient (R^2) value from the fitted multiple regression model was

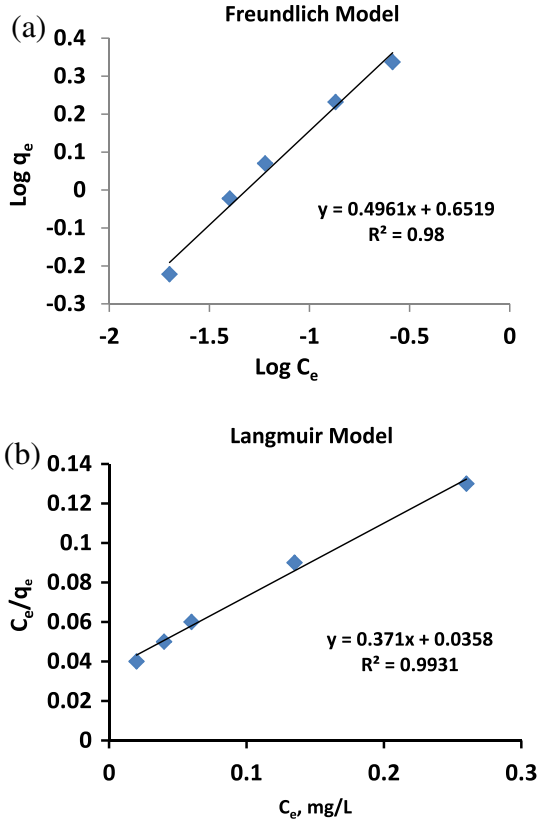

Fig. 8. Linearized a) Freundlich and b) Langmuir isotherms for Cd(II) adsorption on maghemite-magnetite at room temperature.

0.8841, which means that 88.41% of the total variation in Cd removal could be explained by the independent variables in the fitted model. Fig. 9 illustrates the experimental and model predicted values of the Cd percentage removal at different conditions. The correlation coefficient between model predicted values and experimental values was 0.8841 as indicated in Fig. 9. Table 3 shows percentage removal of Cd at different conditions that demonstrate experimental and model predicted values.

3.5. X-ray photoelectron spectroscopy (XPS)

X-ray photoelectron spectroscopy (XPS) studies were carried out to assess the elemental composition and chemical oxidation states of surface and near-surface species. The Casa-XPS software was used to draw and analyze all spectra (Fairley, 2003). XPS wide scan spectra of fresh maghemite-magnetite and Cd adsorbed maghemite-magnetite sorbents are shown in Fig. 10. Four major peaks at binding energies of 281.55, 396.35, 526.55 and 707.15 eV, representing C 1s, N 1s, O 1s, and Fe 2p respectively, are observed for the virgin sorbent (Fig. 10a). Significant changes can be seen in Fig. 10b after Cd(II) adsorption; the peak at binding energy of

Table 1
Multiple regression analysis of Cd percentage removal (dependent variable) against pH, contact time, solid–liquid (*S*/*L*) ratio and temperature of the system (independent variables) for Cd- mixed maghemite-magnetite system.

Square of multiple correlation coefficient (R^2)	Regression coefficients				
	pH, X_1	Contact time in min, X_2	*S*/*L* ratio, X_3	Temperature (°C), X_4	Intercept, *C*
0.8841	21.2095799	0.2992320	42.2337443	−0.7502734	−165.09903

Table 2
Other parameters for model Equation (3.1).

Coefficients:	Std. error	*t* value	Pr(>|*t*|)	Significance level[a]
C (Intercept)	27.46951	−6.010	2.40e-06	***
X_1	2.81835	7.526	5.46e-08	***
X_2	0.02505	11.947	4.62e-12	***
X_3	4.69080	9.004	1.80e-09	***
X_4	0.15945	−4.705	7.32e-04	**

Adjusted *R*-squared: 0.8663.
F-statistic : 49.59 on 4 and 26 DF.
p-value: 8.499e-12.
[a] Significant level codes: 0 '***' 0.001 '**' 0.01 '*' 0.05 '.' 0.1 ' ' 1.

401.25 eV for Cd 3d appears in the Cd(II) loaded sorbent (Fig. 10b and c). (Table 3).

The XPS survey of Fe 2p on the mixed γ-Fe_2O_3–Fe_3O_4 (Fig. 11a) shows two photoelectron peaks centered at 709 and 711–714 eV, indicating the presence of both Fe(II) and Fe(III) at the adsorbent surface. Similar results were reported by Chowdhury et al. (2012). The Fe 2p high resolution spectra were fitted following the example of Pratt et al. (1994) and Chowdhury et al. (2010, 2012) using theoretical multiplet peak (Gupta and Sen, 1975). In the present study, the peak full width at half maximum (FWHM) was found to be between 1.0 and 3.3 eV. Multiplet splitting can occur for more core level photopeaks when the atom contains unpaired valence electrons. Grosvenor et al. (2004) reported that multiplet-splitting of *p* and higher sublevels is complicated due to orbital-angular momentum coupling. According to Hochella (1988), 2p sublevels of transition metals in high-spin or paramagnetic states exhibit considerable line broadening due to complex multiplet splitting phenomena and despite the complexity of these line shapes, spectra of this sort can still be used to determine the oxidation state of the iron in the near-surface of minerals.

The XPS results, shown in Fig. 11, present the theoretical multiplet peaks for iron and Cd adsorbed iron oxide at the surface of the γ-Fe_2O_3 and Fe_3O_4 mixture. Theoretical multiplet analysis of the γ-Fe_2O_3–Fe_3O_4 mixture gave 74.8% of maghemite and 25.2% of magnetite (Fig. 11a). No sharp hematite peak was observed in the XPS spectra. After Cd(II) adsorption on the maghemite-magnetite mixture, it was found that the percent of maghemite decreased to 68.5% (Fig. 11b). At the same time, the percentage of magnetite was increased (Fig. 11b). These results suggest that a redox reaction occurred on the mixed maghemite-magnetite surface when Cd(II) was introduced. Changes in the relative abundance of Fe(II) and Fe(III) in magnetite and maghemite spectra (Fig. 11a and b) upon Cd(II) adsorption are quantitatively elucidated. The data show that in magnetite spectra, the relative content of the Fe(III) and Fe(II)

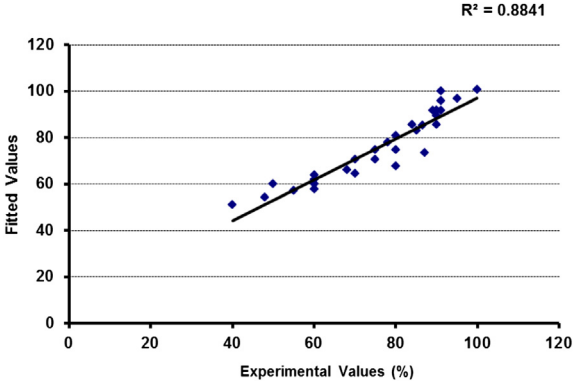

Fig. 9. Percentage removal of Cd at different conditions – (experimental and model predicted values).

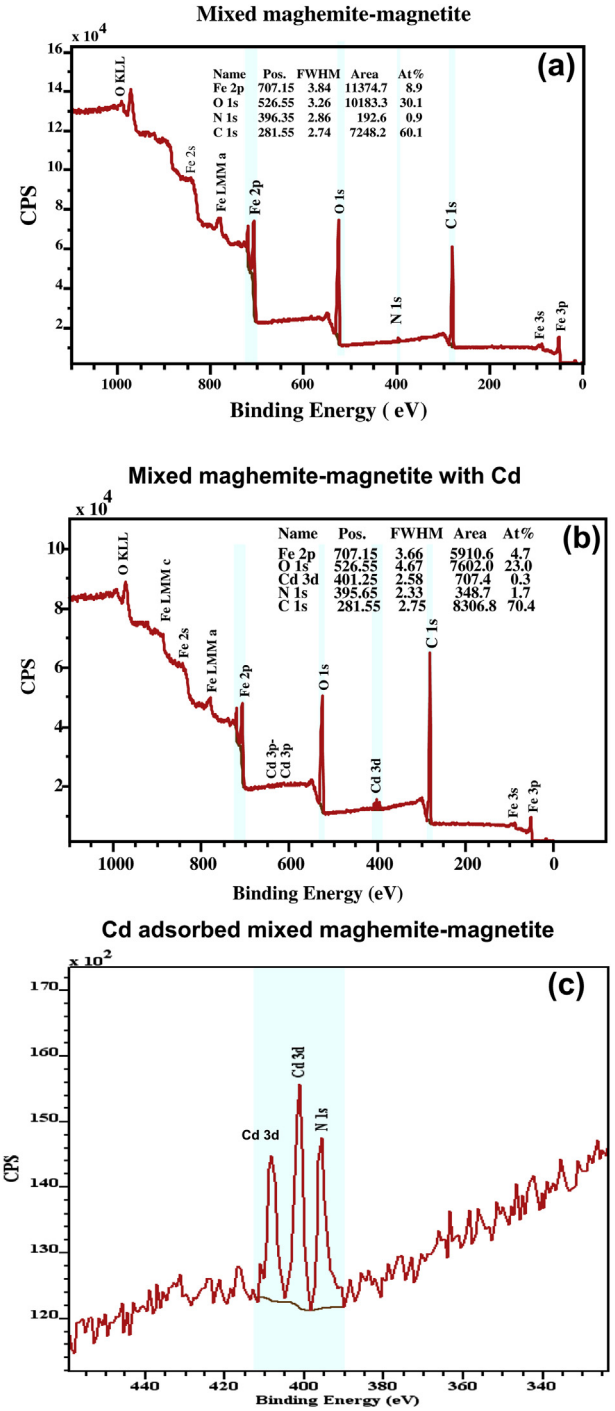

Fig. 10. XPS wide scan spectra of the (a) fresh maghemite-magnetite mixture. (b) Cd(II) loaded maghemite-magnetite mixture. (c) Cd(II) peak on Cd loaded maghemite-magnetite mixture (Binding energy scale in order of descending values).

increases from 17.3 to 21.6% for Fe(III) and 7.9 to 9.9 for Fe(II) indicating the reduction of maghemite in the mixture particles. This indicates reduction at the mixed oxides surface as well as an increase in the amount of magnetite from 25.2% to 31.5%.

The Cd 2d spectrum of the Cd(II) adsorbed sorbent can be found at the peak containing binding energy of 405.06 eV shown in Fig. 12. Additional Auger line has also been observed with MNN group for cadmium at 786.2 eV. The Cd $3d_{5/2}$ peak and Auger parameter analysis suggest the presence of a Cd(II) compound,

Table 3
Percentage removal of Cd at different conditions – (experimental and model predicted values when initial concentration was 1.5 mg/L).

Different pH		Different contact time in min		Different *S*/*L* ratio		Different temperature (°C)	
Experiment-al Cd removal (%)	Predicted values (%)	Experimental Cd removal (%)	Predicted values (%)	Experimental Cd removal (%)	Predicted values (%)	Experimental Cd removal (%)	Predicted values (%)
60	57.38819	40	50.9272	50	59.6482	99.9	100.327
60	63.75107	48	53.9195	60	61.7599	95	96.5754
75	74.35586	55	56.9118	68	65.9833	89	91.3235
80	80.71873	60	59.9042	75	70.2067	84	85.3213
86.5	84.9607	70	64.3926	80	74.430	78	77.8186
90	89.2026	80	67.385	85	82.8768	70	70.3159
90	91.3235	87	73.3696	91	91.3235		
		90	85.3389	91	95.5469		
		90	91.3235	91	99.7703		

possibly a mixture of CdO and $Cd(OH)_2$. The Cd $3d_{5/2}$ peak for the native oxide (polished Cd metal surface, air exposed) was found at 405.06 eV with a FWHM of 1.25 eV (10 eV Pass Energy). The XPS surveys showed that Cd^{2+} ions may undergo oxidation–reduction mechanism upon exposure to mixed maghemite-magnetite as well as the Cd^{2+} ions are most probably fixed by complexation mechanism with the oxygen atoms in the oxy-hydroxyl groups at the shell surface of the iron oxide nanoparticles. Cd(II) may be attracted to the iron oxide surface by adsorption or surface complex formation, which include electrostatic interactions or specific surface bonding. Cd(II) is thus retained on the iron oxide surface by chemical reduction as well as by electrostatic interactions. The amount of cadmium used in the XPS spectrum analysis was very low (0.1–0.4 atomic percent) compared to the amount of iron detected (10–20%) and any iron–Cd complex contribution to the Fe 2p spectrum would be obscured by the large maghemite-magnetite signal.

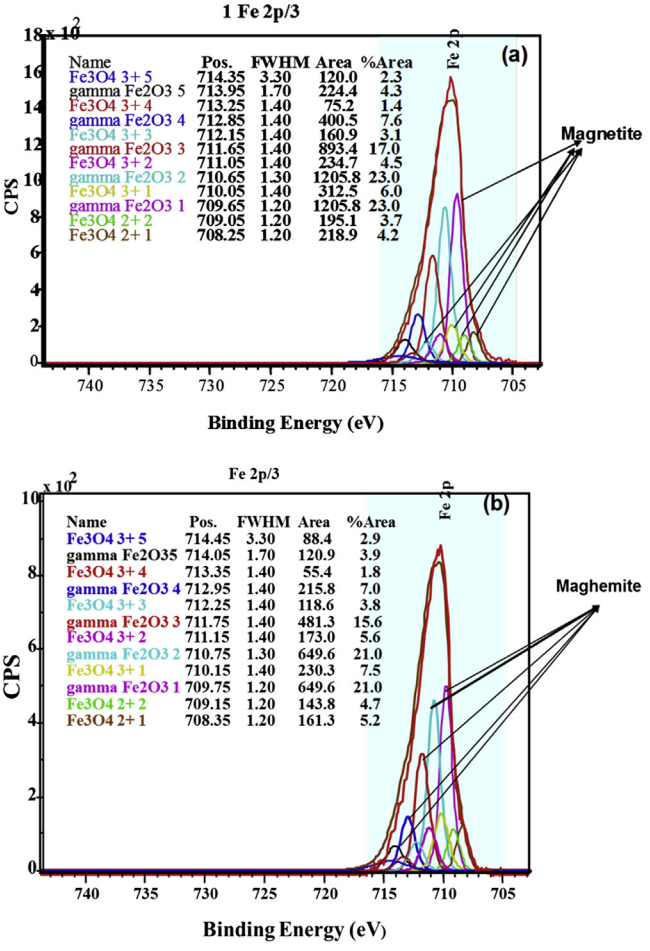

Fig. 11. XPS spectra (a) nano-scale maghemite-magnetite particles and (b) Cd(II)-adsorbed mixed maghemite-magnetite nanoparticles.

4. Conclusions

In the present study, batch adsorption experiments for the adsorption of Cd(II) ions from aqueous solutions have been carried out using mixed maghemite-magnetite as adsorbent. The adsorption characteristics have been examined at different contact times, pH values, initial Cd(II) ion concentrations, and different adsorbent dosage levels. The obtained results can be summarized as follows:

1. The adsorption rate of Cd(II) ions was fast initially, and about 40% of total Cd(II) was removed within 5 min. Thereafter, the adsorption capacity increased slowly with contact time before reaching a plateau after the contact time of 2 h, and then remained constant.
2. Generally, the adsorption capacity of Cd(II) ions by mixed maghemite-magnetite increased with an increase in the pH of the adsorbate solution.
3. With an increase in initial Cd(II) ion concentration, the adsorption capacity of Cd(II) ions on mixed maghemite–magnetite increased but the removal percentage of Cd(II) ions decreased.
4. An increase in adsorbent dosage increased Cd(II) removal but decreased adsorption capacity.
5. Adsorption of Cd(II) ions by mixed maghemite-magnetite was found to follow the pseudo-second-order kinetics model.

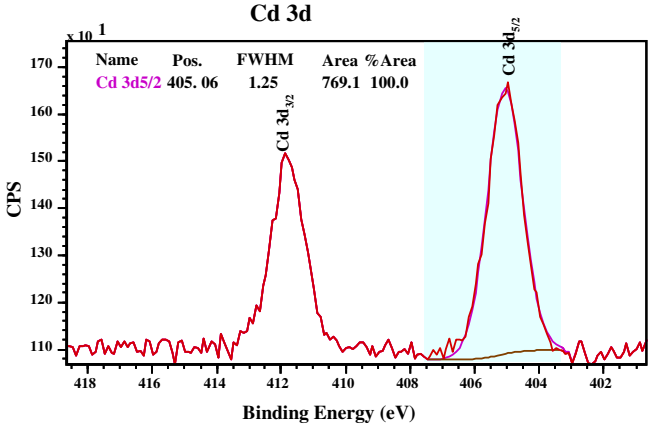

Fig. 12. Cd 3d XPS spectra of Cd(II) loaded maghemite-magnetite mixture. (State background subtracted in data).

6. X-ray photoelectron spectroscopy studies confirmed that Cd^{2+} ions may undergo oxidation-reduction reactions upon exposure to mixed maghemite-magnetite, or may become fixed by complexation with oxygen atoms in the oxy-hydroxy groups at the shell surface of the iron oxide nanoparticles. Theoretical multiplet analysis identified the γ-Fe_2O_3– Fe_3O_4 mixture to comprise 74.8% of maghemite and 25.2% of magnetite (Fig. 11a). Following Cd(II) adsorption by the maghemite-magnetite mixture, the percent maghemite decreased from 74.8 to 68.5% (Fig. 11b).
7. Batch adsorption studies indicate that mixed maghemite-magnetite has strong adsorption towards Cd(II) ions. The results of the present work show that 0.8 g/L of 20–60 nm maghemite-magnetite particles removed up to 1.5 mg/L Cd, and the approximate cost of this nano-scale adsorbent is $225/kg (Reade Advance Materials, 2009). Thus the cost of using nano maghemite-magnetite particles adsorbent would be $0.18/L. To take advantage of this, maghemite-magnetite particles can be used in water treatment and site remediation to control or minimize exposure to living organisms. Mixed maghemite-magnetite particles can also be used in the design of permeable reactive barriers for subsurface remediation. Permeable reactive barriers containing maghemite-magnetite particles could be constructed for in situ remediation of groundwater contaminated with heavy metals. To develop a decision framework for helping utilities determine the most appropriate adsorbent based on cost and performance, more research and investigations are necessary to determine the applicability of mixed iron oxide particles in the construction of permeable reactive barriers.

Acknowledgements

The research presented in this paper has been funded by an Individual Discovery Grant from the Natural Sciences and Engineering Research Council of Canada awarded to Dr. E.K. Yanful. The authors are grateful to Dr. A. Pratt of CANMET Mining and Mineral Sciences Laboratories for his suggestions.

References

Alloway, B.J., Steinnes, E., 1999. Anthropogenic additions of cadmium to soils. In: McLaughlin, M.J., Singh, B.R. (Eds.), Cadmium in Soils and Plants. Kluwer Academic Publishers, Boston.
Barkat, M., Nibou, D., Chegrouche, S., Mellah, A., 2009. Kinetics and thermodynamic studies of chromium(VI) adsorption onto activated carbon from aqueous solutions. Chem. Eng. Process. 48, 38–47.
Boparai, H.K., Joseph, M., Caroll, D.M., 2009. Kinetics and thermodynamics of cadmium ion removal by adsorption onto nano zerovalent iron particles. J. Hazard. Mater. 186, 458–465.
Chowdhury, S.R., Yanful, E.K., 2010. Arsenic and chromium removal by mixed magnetite–maghemite nanoparticles and the effect of phosphate on removal. J. Environ. Manage. 91, 2238–2247.
Chowdhury, S.R., Yanful, E.K., Pratt, A.R., 2012. Chemical states in XPS and Raman analysis during removal of Cr(VI) from contaminated water by mixed maghemite–magnetite nanoparticles. J. Hazard. Mater. 235–236, 246–256.
Cornell, R., Schwertmann, U., 2003. The Iron Oxides: Structure, Properties, Reactions, Occurrence and Uses. Willey-VCH, Weinheim.
Erhan, D., Kobya, M., Ehf, S., Ozkan, T., 2004. Adsorption kinetics for Cr (Vi) removal from aqueous solution on activated carbon prepared from agro wastes. J. Water 30 (4), 533–541.
Fairley, N., 2003. CasaXPS Version 2.2.19.
Gavaskar, A., Tatar, L., Condit, W., 2005. Cost and Performance Report Nanoscale Zero-valent Iron Technologies for Source Remediation. Naval Facilities Engineering Command (NAVFAC). Contract report: CR-05-007-ENV.
Geological Survey of Japan, 2005. Atlas of Eh-pH Diagrams – Intercomparison of Thermodynamic Databases. National Institute of Advanced Industrial Science and Technology. Open File Report No.419.
Grosvenor, P.A., Kobe, B.A., Biesinger, M.S., McIntyre, N.S., 2004. Investigation of multiplet splitting of Fe 2p XPS spectra and bonding in iron compounds. Surf. Interface Anal. 36, 1564–1574.
Gupta, R.P., Sen, S.K., 1975. Calculation of multiplet structure of core *p* -vacancy levels. Phys. Rev. 12, 15–19.
Ho, Y.S., McKay, G.., Wase, D.A.J., Foster, C.F., 2000. Study of the sorption of divalent metal ions on to peat. Adsorp. Sci. Technol. 18, 639–650.
Hochella, M.F., 1988. Auger electron and X-ray photoelectron spectroscopies. Rev. Mineral. Geo-chem. 18, 573–637.
Li, H., Zhou, Q., Wu, Y.F.J., Wang, T., Jiang, G., 2009. Effects of waterborne nano-iron on medaka (*Oryzias latipes*): antioxidant enzymatic activity, lipid peroxidation and histopathology. Ecotoxicol. Environ. Saf. 72 (3), 684–692.
Mahalik, M.P., Hitner, H.W., Prozialeck, W.C., 1995. Teratogenic effects and distribution of cadmium (Cd^{2+}) administered via osmotic minipumps to gravid Cf-1 mice. Toxicol. Lett. 76, 195–202.
Martin, A.B.P., Zapata, V.M., Aguilar, O.M., Saez, J., Lorens, M.L., 2007. Removal of cadmium from aqueous solutions by adsorption onto orange waste. J. Hazard. Mater. 139, 122–131.
Moore, J.W., Ramamoorthy, S., 1984. Heavy Metals in Natural Waters. Springer-Verlag New York Inc, ISBN 3-540-90885-4.
Naidu, R., Bolan, N.S., Kookana, R.S., Tiller, K.G., 1994. Ionic-strength and pH effects on the sorption of cadmium and the surface charge of soils. Eur. J. Soil Sci. 45, 419–429.
Pang, S.C., Chin, S.F., Anderson, M.A., 2007. Redox equilibria of iron oxides in aqueous-based magnetite dispersions: effect of pH and redox potential. J. Colloid Interface Sci. 311, 94–101.
Phenrat, T., Long, T.C., Lowry, G.V., Veronesi, B., 2009. Partial oxidation ("aging") and surface modification decrease the toxicity of nanosized zerovalent iron. Environ. Sci. Technol. 43, 195–200.
Pratt, A.R., Muir, I.J., Nesbitt, H.W., 1994. X-ray photoelectron and Auger electron spectroscopic studies of pyrrhotite and mechanism of air oxidation. Geochim. Cosmochim. Acta 58, 827–841.
Santiago, V.R., Fedkin, M.V., Lvov, S.N., 2012. Protonation enthalpies of metal oxides from high temperature electrophoresis. J. Colloid. Interface. Sci. 371, 136–143.
Sharma, Y.C., 2008. Thermodynamics of removal of cadmium by adsorption on an indigenous clay. Chem. Eng. J. 145, 64–68.
Singh, D.B., Rupainwar, D.C., Prasad, G., Jayaprakas, K.C., 1998. Studies on the Cd (II) removal from water by adsorption. J. Hazard. Mater. 60, 29–40.
Srivastava, S.K., Tyagi, R., Pant, N., 1989. Adsorption of heavy metal ions on carbonaceous material developed from the waste slurry generated in local fertilizer plants. Water Res. 23, 1161–1165.
Stumn, W., 1987. Aquatic Surface Chemistry – Chemical Process at the Particle-water Interface. Wiley, NewYork.
Tan, G.Q., Xiao, D., 2009. Adsorption of cadmium ion from aqueous solution by ground wheat stems. J. Hazard. Mater. 164, 1359–1363.
Tuutijärvi, T., Sillanpääa, J.L.M., Chenb, G., 2009. As(V) adsorption on maghemite nanoparticles. J. Hazard. Mater. 166, 1415–1420.
Waalkes, M.P., 2000. Cadmium carcinogenesis in review. J. Inorg. Biochem. 79, 241–244.
Wang, F.Y., Wang, H., Ma, J.W., 2010. Adsorption of Cd(II) ions from aqueous solution by a new low-cost adsorbent-Bamboo charcoal. J. Hazard. Mater. 177, 300–306.
Weber, W.J., Asce, J.M., Morris, J.C., 1963. Kinetics of adsorption on carbon from solutionProceedings of the American Society of Civil Engineers. J. Sanit. Eng. Div. 89, 31–59.
WHO, 2008. Guidelines for Drinking Water Quality: Recommendations, third ed., vol. 1. World Health Organisation, Geneva.
Yang, C.H., 1998. Statistical mechanical study on the Freundlich isotherm equation. J. Colloid Interface Sci. 208, 379–387.
Yean, S., Cong, L., Yavuz, C.T., Mayo, J.T., Yu, W.W., 2005. Effect of magnetite particle size on adsorption and desorption of arsenite and arsenate. Mater. Res. Society. J. Mater. Res. 20 (12), 3255–3264.